EurJIC
European Journal of Inorganic Chemistry

A Journal of ChemPubSoc Europe

Accepted Article

Title: Ruthenium(II)-Arene Metallacycles: Crystal Structures, Interaction with DNA and Cytotoxicity

Authors: Hongke Liu, Hongyan Wang, Yong Qian, Fang-xin Wang, Abraha Habtemariam, Zong-Wan Mao, and Peter J Sadler

To be cited as: *Eur. J. Inorg. Chem.* 10.1002/ejic.201601226

Link to VoR: http://dx.doi.org/10.1002/ejic.201601226

WILEY-VCH

Ruthenium(II)-Arene Metallacycles: Crystal Structures, Interaction with DNA and Cytotoxicity

Hong-Yan Wang,[a] Yong Qian,*[a] Fang-Xin Wang,[b] Abraha Habtemariam,[c] Zong-Wan Mao,*[b] Peter J. Sadler,*[c] Hong-Ke Liu*[a]

Abstract: A series of 24, 26-membered $Ru(II)_2$ metallamacrocycles containing 1-(3-((1H-imidazol-1-yl)methyl)benzyl)-1H-imidazole (*m*-bib) and 1-(4-((1H-imidazol-1-yl)methyl)benzyl)-1H-imidazole (*p*-bib) ligands have been synthesized and characterized. X-ray crystal structures of $[Ru_2(\eta^6\text{-}p\text{-cymene})_2(m\text{-bib})_2Cl_2](CF_3SO_3)_2$ (**2**), $[Ru_2(\eta^6\text{-}p\text{-cymene})_2(m\text{-bib})_2Cl_2](SbF_6)_2$ (**3**), $[Ru_2(\eta^6\text{-}p\text{-cymene})_2(m\text{-bib})_2I_2]I_2$ (**6**), and $[Ru_2(\eta^6\text{-}p\text{-cymene})_2(p\text{-bib})_2Cl_2](CF_3SO_3)_2$ (**8**) were determined and found to exhibit chair-like conformations. In general, the complexes exhibited little or moderate anti-proliferative activity towards cancer cells (human lung cancer cells (A549), breast adenocarcinoma cells (MCF-7), cervical epithelioid carcinoma cells (HeLa)) as well as normal liver cells (L02), except $[Ru_2(\eta^6\text{-}p\text{-cymene})_2(p\text{-bib})_2Cl_2](NO_3)_2$ (**10**) (IC_{50} = 16.7 μM) which had activity comparable with the anticancer drug cisplatin (IC_{50} = 15.8 μM). Gel electrophoresis studies suggested that the complexes can interacted with DNA and induce DNA condensation.

Introduction

Transition metal complexes play an important role in the design of metal-based drugs,[1] providing a variety of coordination numbers and geometries,[2] the diversity of linking ligands,[3] and structures.[4] The square-planar complex cisplatin in particular is now widely used for the treatment of ovarian, head and neck, bladder, cervical and lymphomas cancers.[5] However, the clinical use of cisplatin still has some limitations including drug resistance and side effects, e.g. neurotoxicity and gastrointestinal toxicity.[6] Ruthenium-based complexes, are potential anticancer metal-based candidates,[7] showing promising activity.[8] KP1019[9] has been in phase II clinical trials. Ruthenium(II)-arene complexes have been shown promising *in vitro* or *in vivo* biological activity in various studies.[10] Half-sandwich ruthenium(II)-arene complexes of the general type $[Ru(\eta^6\text{-arene})(YZ)X]^{n+}$ have also attracted attention as potential anticancer drugs.[11] The monodentate ligand X and chelated YZ of these "piano-stool" structures have an important influence on the antiproliferative activity.[12] The leaving group X affects the hydrolysis and then affects the cytotoxicity towards cancer.[13] Changes in YZ also have significant effects on anticancer activities.[14] Moreover, dinuclear/multinuclear ruthenium(II)-arene complexes generally displayed more potential cytotoxic activity comparing with mononuclear complexes.[15-17] Thus, they provide us a path for fine-tuning the structure of complexes, and further developing novel potential anticancer organometallic complexes based on structure−activity relationships.[18]

DNA in cancer cells is a target for some classes of ruthenium(II)-arene complexes.[19] These complexes can bind directly to DNA bases especially guanine, and also intercalate into DNA when the arene is extended and generate adducts which inhibit cell division[17] and proliferation.[12,20-21] Linking Ru(II) arene centres can endow multinuclear complexes have new modes of interaction with DNA. Modification of the ligands or bridging linkers can lead to significant differences in anticancer activity and different types of DNA binding modes.[22] For example, the ligands containing N-donors (e.g. polypyridine ligands) and their derived complexes of general type $[(\eta^6\text{-arene})RuX(K^2\text{-N,N-L})]Y$ display promising anticancer activity.[23] We report herein the synthesis and characterization of a series of novel metallacyclic diruthenium(II)-arene complexes containing flexible bidentate imidazole ligands *m*-bib or *p*-bib, and their antiproliferative activities have been evaluated. The binding of these diruthenium metallamacrocycles to DNA has been investigated by gel electrophoresis. Metallacyclic dinuclear ruthenium complexes offer the potential for new anticancer agents with novel modes of binding to DNA.

Results and Discussion

Design and Synthesis of Macrocyclic Diruthenium Complexes (1-12)

Two flexible ligands 1-(3-((1H-imidazol-1-yl)methyl)benzyl)-1H-imidazole (*m*-bib), 1-(4-((1H-imidazol-1-yl)methyl)benzyl)-1H-imidazole (*p*-bib) were prepared according to previous reports.[24] Macrocyclic diruthenium complexes (**1**, **2**, **7** and **8**) were obtained from the direct reaction of the appropriate ligands (*m*-bib or *p*-bib) with the dimer $[Ru(\eta^6\text{-}p\text{-cymene})Cl_2]_2$ (Scheme 1), complexes (**3**-**6** and **9**-**12**) were prepared by treating complexes $[Ru_2(\eta^6\text{-}p\text{-cymene})_2(m\text{-bib})_2Cl_2](Cl)_2$ (**1**) or $[Ru_2(\eta^6\text{-}p\text{-cymene})_2(p\text{-bib})_2Cl_2](Cl)_2$ (**7**) with appropriate metal salt.[25] All complexes were obtained in good yields and characterized by ^1H NMR spectroscopy, mass spectrometry, and elemental analysis (see Experimental section and supporting information for full details).

X-ray Crystallography

The crystal structures of 4 diruthenium-arene complexes (**2**, **3**, **6** and **8**) were determined by X-ray crystallographic method. These complexes contain two ruthenium(II) centers linked by two flexible ligands (Figures 1-4). Details of data collection,

[a] Hong-Yan Wang,[a] Yong Qian,[a]* Hong-Ke Liu[a]*
Jiangsu Collaborative Innovation Center of Biomedical Functional Materials, Jiangsu Key Laboratory of Biofunctional Materials, College of Chemistry and Materials Science, Nanjing Normal University,
Nanjing, 210046,Jiang Su, P. R. China
E-mail: liuhongke@njnu.edu.cn, yongqian@njnu.edu.cn
[b] Fang-Xin Wang[b], Zong-Wan Mao[b]*
School of Chemistry, Sun Yat-Sen University,
Guangzhou, 510275,Guang Dong, P. R. China
E-mail:cesmzw@mail.sysu.edu.cn
[c] Peter J. Sadler[c]*
Department of Chemistry, University of Warwick,
Gibbet Hill Road, Coventry CV4 7AL, UK.
E-mail:P.J.Sadler@warwick.ac.uk

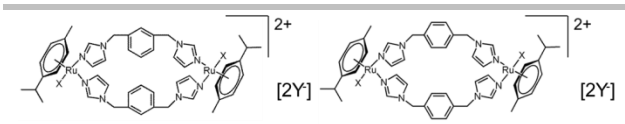

complex	X	Y
1	Cl	Cl
2	Cl	CF_3SO_3
3	Cl	SbF_6
4	Cl	NO_3
5	Br	Br
6	I	I

complex	X	Y
7	Cl	Cl
8	Cl	CF_3SO_3
9	Cl	SbF_6
10	Cl	NO_3
11	Br	Br
12	I	I

Scheme 1. Structures of metallamacrocyclic diruthenium complexes.

structure solutions, and refinement are given in Table S1, and selected bond lengths and angles are shown in Table S2.

Complex **2** crystallized in a triclinic *P*$\bar{1}$ space group, and showed a classic "chair-like" metallamacrocyclic structure with $CF_3SO_3^-$ counter anions (Figure 1). Two *m*-bib ligands link the two ruthenium centres. Each Ru was coordinated by two N atoms from two ligands (*m*-bib) and one Cl atom. The two imidazole groups are located on the opposite faces of the central aromatic ring forming a *trans* conformation. The bond lengths of Ru-N and Ru-Cl are 2.111(6) Å, 2.135(6) Å, and 2.4315(17) Å, respectively, and angles N1a-Ru1-Cl1, N1a-Ru1a-N4, N4-Ru1-Cl1 are 85.32(16)°, 83.3(2)°, 88.01(16)°, respectively. The $CF_3SO_3^-$ anion is located outside of the "Ru_2L_2" metallamacrocycle. The fluorine atoms of $CF_3SO_3^-$ form hydrogen bonds (C-H···F) with a C atom on the methylene of the *m*-bib ligand, with C---F distance of 3.10 Å (Table S3). *π*−*π* interactions are present between two paralleled phenyl rings from two adjacent units with a "center-to-center" distance of 3.71 Å. The packing of "Ru_2L_2" units is shown in Figure 1d.

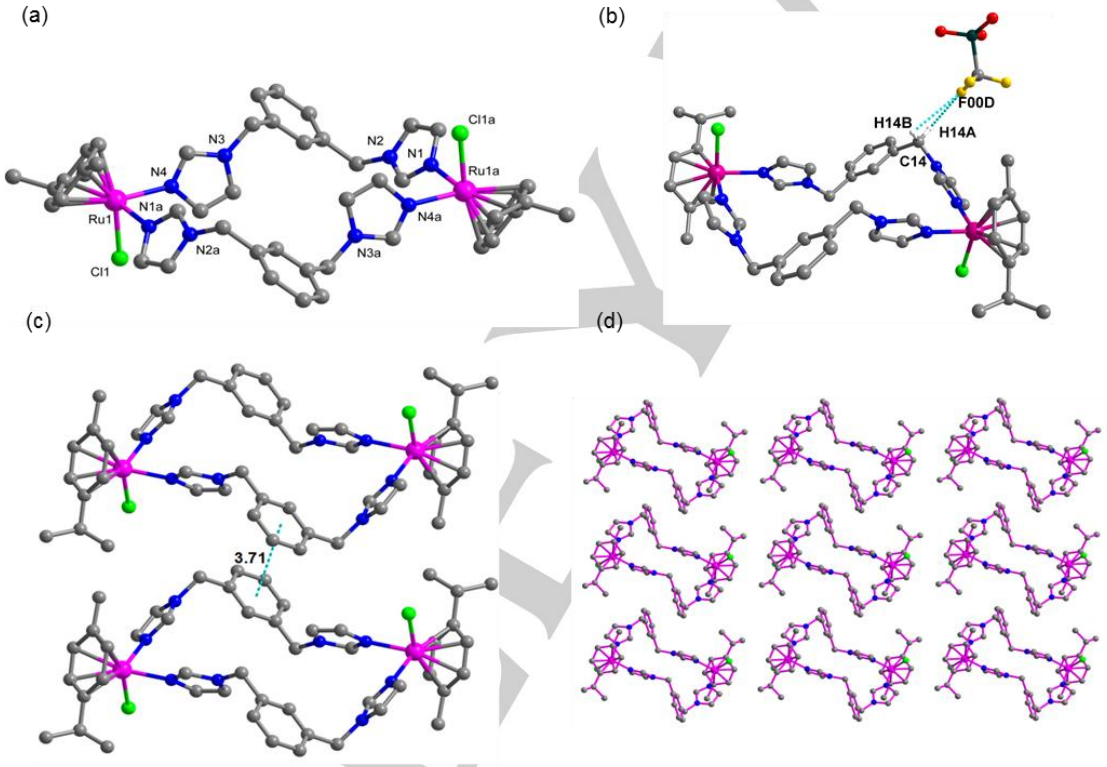

Figure 1. (a) X-ray crystal structure of **2**. (b) Hydrogen bonds (C–H···F) between $CF_3SO_3^-$ and the unit "Ru_2L_2". (c) The π-π stacking interactions between two parallel phenyl rings of two adjacent units, with a "centre-to-centre" distance of 3.71 Å. (d) The packing of the "Ru_2L_2" units of **2**. Counter anions, solvent molecules and hydrogen atoms have been omitted for clarity.

Complex **3** showed a similar structure to that of complex **2**, in which each Ru atom coordinated by two N atoms from two *m*-bib ligands and one Cl atom, forming a slightly distorted metallamacrocyclic structure (Figure 2). The SbF_6^- anions are located outside of metallamacrocycle. There are different types of H-bonds between F atoms of SbF_6^- and η^6-*p*-cymene ligand. One type of H-bond (C1-H1···F1) is between F1 atom and a C atom on the methyl group of η^6-*p*-cymene ligand, another type of H-bond (C2-H2···F2) is between F2 atom and a C atom from benzene ring of η^6-*p*-cymene ligand. The C1---F1 and C2---F2 distances are 3.28 Å, and 3.38 Å, respectively. Hydrogen bonds between the F3 atom and η^6-*p*-cymene ligand are also observed (C3-H3···F3, C4-H4···F3) with bond lengths of 3.48 Å or 3.30 Å, respectively (Table S3). It is noteworthy that 3 fluorine atoms of SbF_6^- connect two Ru_2L_2 units by hydrogen bonds, forming a two-dimensional network, in which the Ru_2L_2 units have two different orientations.

Complex **6** was obtained by treating **1** with KI in methanol and its yellow crystals were suitable for X-ray analysis. Complex **6** also crystallized in the monoclinic $P2_1/c$ space group, each ruthenium centre is coordinated by an Iodine atom and two N atoms from two *m*-bib ligands, forming a "chair-like" metallamacrocyclic (Figure 3).

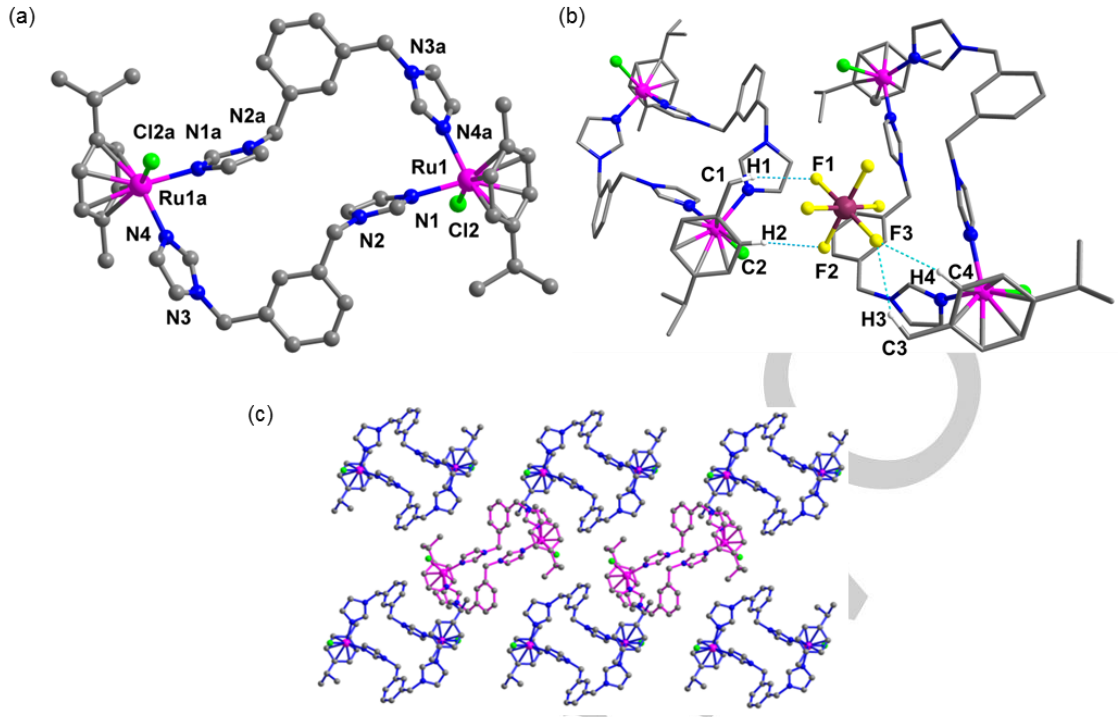

Figure 2. (a) X-ray crystal structure of **3**. (b) Hydrogen bond (C–H···F) between SbF_6^- and the unit "Ru_2L_2". (c) The packing of the "Ru_2L_2" units of **3**. Counter anions, solvent molecules and hydrogen atoms have been omitted for clarity.

The Ru_2L_2 units of **6** show two different orientations in the packing structure (Figure 3b).

The structure of complex **8** containing the *p*-bib ligands was determined by single crystal X-ray diffraction (Figure 4). **8** crystallized in an orthorhombic $P2_12_12_1$ space group, forming a metallamacrocyclic structure with two *p*-bib ligands and two Ru atoms. Each Ru atom is coordinated by one Cl atom and two N atoms from two ligands. The Ru-N bond lengths range from 2.091(13) Å to 2.129(13) Å, and the Ru-Cl bond lengths from 2.411(4) Å to 2.426(4) Å. These bond lengths are slightly shorter than those in the Ru(II) arene *m*-bib structures (**2**, **3** and **6**). The angles N-Ru-N range from 86.6(5)° to 89.7(5)°, and N-Ru-Cl from 84.3(4)° to 88.3(4)°, similar to those of the *m*-bib complexes. H-bonds are formed between $CF_3SO_3^-$ anion and three surrounding Ru_2L_2 units. As shown in the Figure 4b, the representative H-bonds around $CF_3SO_3^-$ anion include those between the C-H from the methylene of *p*-bib ligand and F1 atom (C1-H1···F1), the C-H from the isopropyl group of η^6-*p*-cymene and F2 atom (C2-H2···F2), between the C-H from the imidazole of *p*-bib ligand and F3 atom (C3-H3···F3), with C---F distances of 3.24 Å, 3.36 Å or 3.25 Å, respectively (Table S3). The Ru_2L_2 units of **8** also show two different orientations in the packing structure (Figure 4c). These results indicate that Ru_2L_2 metallamacrocyclic complexes can be obtained by reaction of dimer $[Ru(\eta^6\text{-p-cymene})Cl_2]_2$ with flexible bidentate imidazole ligands *m*-bib or *p*-bib. These metallamacrocyclic complexes adopt the "chair-like" conformation with the two coordinated halogen atoms X (Cl, or I) located on the opposite sides of the macrocyclic ring.

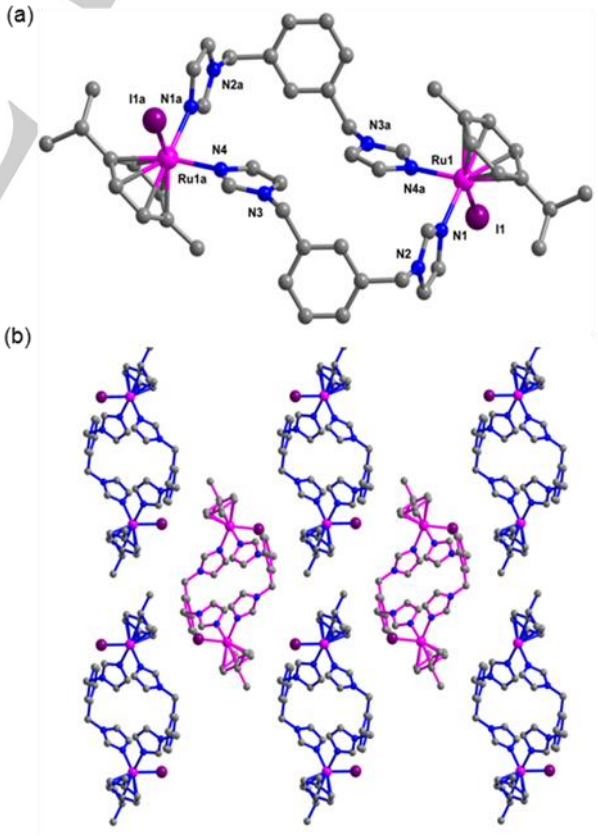

Figure 3. (a) X-ray crystal structure of **6**. (b) The packing of the "Ru_2L_2" units of **6**. Solvent molecules and hydrogen atoms have been omitted for clarity.

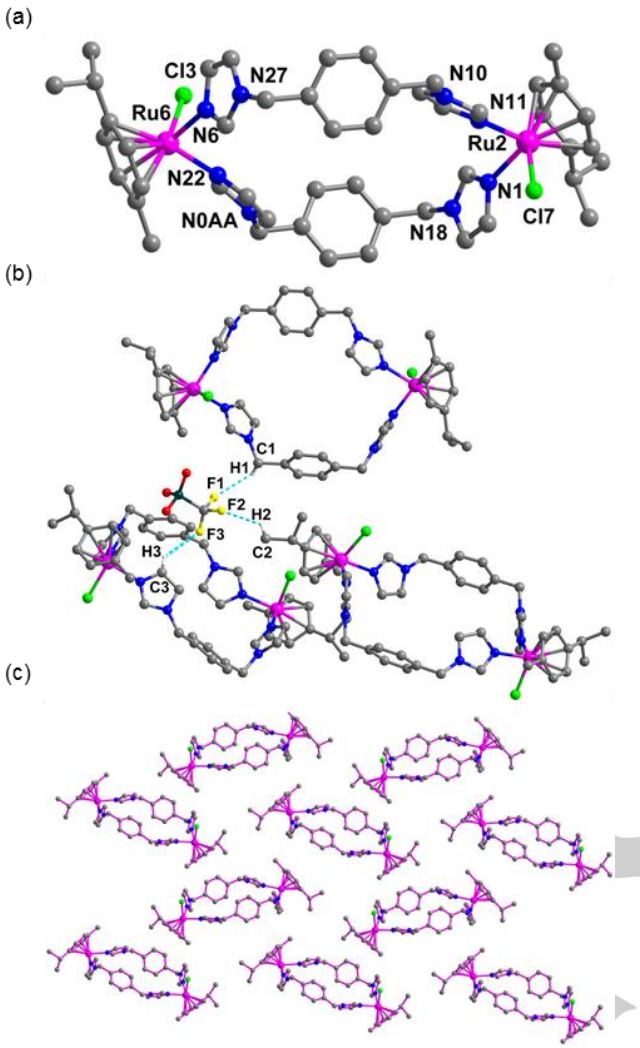

Figure 4. (a) X-ray crystal structure of **8**. (b) 3 different types of hydrogen bonds between $CF_3SO_3^-$ and the "Ru_2L_2" unit. (c) Two packing modes for **8**. Counter anions, solvent molecules and hydrogen atoms have been omitted for clarity.

Anticancer activity assays

The anti-proliferative activities of complexes **1**−**12** were investigated in three cancer cell lines: human lung cancer cell line (A549), human breast adenocarcinoma cell line (MCF-7), and human cervical epithelioid carcinoma (HeLa) as well as a human normal liver cell line (L02) (Table S4). The cytotoxicity was determined by the MTT assay after 44 h of exposure to the complexes. The IC_{50} values are summarized in Table S4. Complexes **1**-**5**, **7**-**9**, **11**-**12** were nontoxic (IC_{50}>100 μM) towards the human normal liver cell line (L02). **10** shows much higher anti-proliferative activity to the cancer cells than the other complexes, with IC_{50} values ranging from 16.7 μM to 30.1 μM, and **10** is more active towards cancer cells than towards the human normal L02 cell line (35.6 μM). Potency towards HeLa cells decreased in the order **4**>**3**>**5**>**1**>**6**>**2** for the *m*-bib ligand and in the order **10**>**9**>**7**>**12**>**8**>**11** for the *p*-bib ligand. Additionally, the data obtained from MTT assay clearly indicate that all the complexes except **10** show low cytotoxicity (IC_{50}>100 μM) towards MCF-7, and A549 cell lines. Complex **11** displays good cytotoxicity towards the A549 cell line (43.9±1.4 μM) compared with other cell lines (IC_{50}>200 μM). The anti-proliferative activity of **10** towards the HeLa cell line (IC_{50}=16.7 μM) is comparable with that of the anticancer drug cisplatin (IC_{50}=15.8 μM). Based on these results, it would appear that the specific molecular shape, the chemical structure, and the nature of anion may play important roles in the cytotoxicity of these complexes.

Solubility studies

All the complexes can be dissolved in DMSO, CH_3OH, 5% DMSO/95% H_2O, and complexes can also be dissolved in CH_2Cl_2, $CHCl_3$ except that complexes with iodide ligand are only slightly soluble. However, the solubility of the complexes in water differs, decreasing in the order **1**>**2**>**4**>**5**>**6**≈**3** for the *m*-bib ligand and in the order **7**>**8**>**10**>**11**>**12**>**9** for the *p*-bib ligand (Figure S1 in Supporting Information).

DNA electrophoresis studies

Gel electrophoresis assays were used for further studies of the interaction between DNA and these ruthenium(II) macrocycles. Positively-charged ruthenium complexes can usually bind to negatively charged DNA, [7b, 26] so we expected that the binding of closed circular DNA to these macrocyclic ruthenium complexes would result in decreasing the migration rate of supercoiled plasmid (Form II) in agarose gel electrophoresis and formation of a new band for condensed DNA (Form I), as reported in other studies.[26a] As shown in the Figures 5 and S2, it was clear that the condensation of supercoiled pBR322 DNA occurs in the presence of complexes **1**, **4**, **5**, **6**, **7**, **10**, **11** and **12**. With the increasing mol ratio of complexes, the extent of condensation Form I bands increased and the density of supercoiled bands (Form II) decreased. These results indicate that dinuclear ruthenium complexes **1**, **4**, **5**, **6**, **7**, **10**, **11** and **12** can significantly affect the structure of the supercoiled DNA, that probably could lead to distortions of nuclear DNA and cell death.[7b,27,28]

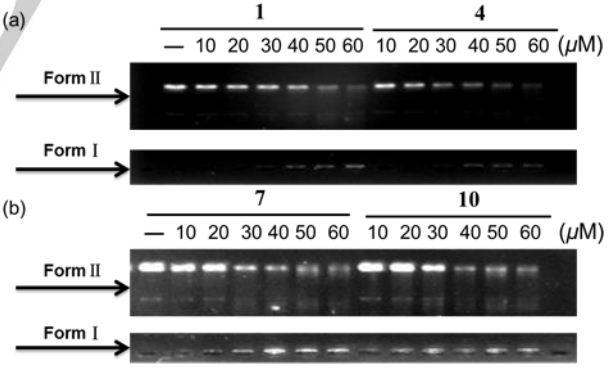

Figure 5. (a) Agarose gel electrophoresis bands for supercoiled pBR322 plasmid DNA (10 μM) after incubation with complexes **1** and **4** , and (b) complexes **7** and **10** in PBS buffer (100 mM) at 310 K for 12 h. Complex concentrations are 10, 20, 30, 40, 50 and 60 μM.

Stability studies

To investigate the stability of complexes, **1**, **5**, **6**, **7**, **11**, **12** were monitored in 5% DMSO/95% H_2O (v/v) at 298 K by UV-vis spectroscopy. As shown in Figure S3, the absorption spectra of **1**, **5**, **6**, **7**, **11**, **12** show only little or no change with time, indicating that these complexes are stable in aqueous solution at 298 K.

Cellular uptake studies

In order to investigate whether intracellular ruthenium concentration correlate with cytotoxicity, intracellular concentration of ruthenium was determined by inductively coupled plasma mass spectrometry (ICP-MS). After incubation with 20 μM complexes for 24 h, the intracellular ruthenium concentrations are shown in Figure 6. Lipophilicity, molecular size and many other aspects may influence the cellular uptake as previously suggested.[29-31] The Ru content from **1**, **4**, **5**, **6**, **7**, **10**, **11** and **12** in HeLa cells decreases in the order **1**>**5**>**6**=**4** and **7**>**11**>**12**>**10** for complexes with the *m*-bib and *p*-bib ligand, respectively. Interestingly, the trend of intracellular ruthenium concentrations does not correlate with their cytotoxicity. For instance, the higher intracellular ruthenium concentration of **7** was not matched by higher cytotoxicity compared with other complexes.

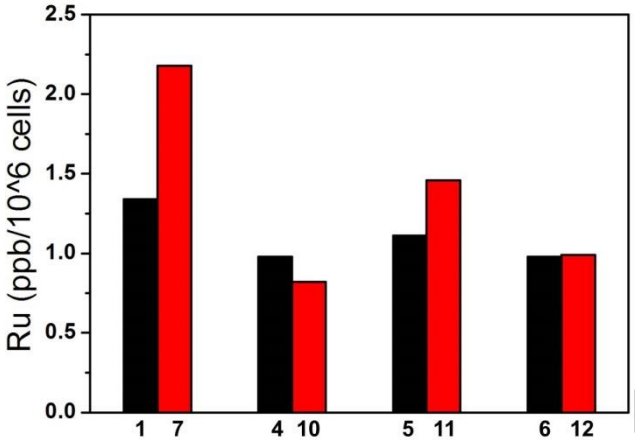

Figure 6. The concentration of Ru in HeLa cells after exposing to 20 μM of complexes **1**, **4**, **5**, **6**, **7**, **10**, **11** and **12** for 24 h in a drug-free medium.

Conclusions

In summary, 12 new metallamacrocyclic Ru_2L_2 complexes containing two either *m*-bib or *p*-bib imidazole ligands have been synthesized and characterized. Single crystal structure analyses showed that these complexes were diruthenium-arene Ru_2L_2 metallacycles with a *trans* conformation, a "titled chair". Gel electrophoresis studies revealed that they can affect the structure of supercoiled DNA significantly, and induce DNA condensation. Furthermore, complex **10** exhibited antiproliferative activity toward HeLa cancer cell line comparable with that of cisplatin (Table S4). Further studies will focus on the chemical and biochemical reactivity of these metallamacrocycles and the mechanism of anticancer activity.

Experimental Section

Materials and methods

All chemicals used in this work were purchased from commercial sources and used without further purification. The dimer [Ru(η^6-*p*-cymene)Cl_2]$_2$ and two ligands 1-(3-((1H-imidazol-1-yl)methyl)benzyl)-1H-imidazole (*m*-bib), 1-(4-((1H-imidazol-1-yl)methyl)benzyl)-1H-imidazole (*p*-bib) were prepared according to literature procedures.[24] The ruthenium complexes were prepared according to literature procedures.[25] ^{1}H NMR spectra were recorded on a Bruker Avance II 400 spectrometer at 298 K. The chemical shifts are reported in parts per million (ppm) and referenced to residual signals of deuterated solvents. Electrospray ionization mass spectra (ESI-MS) were obtained on a Mass Lynx operating system. Elemental analyses (C, H, N) were performed with a Perkin-Elmer 240C elemental analyzer. UV/Vis spectra were recorded on a Varian Cary 50 spectrophotometer. The X-ray crystallographic data were collected on a Bruker Smart Apex II CCD Diffractometer using graphitemonochromatized Mo-K_α radiation (λ= 0.71073 Å) from a rotatinganode generator. Gel electrophoresis was performed on a DYY-2C gel electrophoresis spectrometer. Agarose gel electrophoresis of pBR322 DNA was visualized using the gel imaging system (RAD ChemiDox XPS, American)

Synthesis of complexes

Synthesis of [Ru_2(η6-*p*-cymene)$_2$(*m*-bib)$_2Cl_2$]Cl_2 (1)

To a stirring solution of [$RuCl_2$(η^6-*p*-cymene)]$_2$ (61.2 mg, 0.1 mmol) in MeOH (12 mL), a solution of the ligand *m*-bib (47.8 mg, 0.2 mmol) in MeOH (3 mL) was added dropwise under argon. The resulting mixture was stirred at 338 K for 12 h. The solvent was removed under reduced pressure by a rotary evaporator to give a crude product. Purification by flash column chromatography using CH_2Cl_2/MeOH elution mixture afforded the product as a yellow solid (40.6 mg, yield 37.2%). ^{1}H NMR ($CDCl_3$, 400 MHz) δ: 9.41 (2H, s, H_{im}), 9.26 (2H, s, H_{im}), 8.15 (2H, s, H_{im}), 7.49 (4H, d, H_{im}), 6.85 (8H, m, H_{bz}, *m*-bib), 6.50 (2H, d, H_{im}), 5.92 (8H, d, H_{bz}, *p*-cymene), 5.39 (4H, d, CH_2), 4.94 (4H, d, CH_2), 2.51 (2H, m, CH), 1.89 (6H, s, CH_3), 1.16 (12H, d, CH_3). ESI-MS(+): calcd for [**1**-2Cl^-]$^{2+}$ *m/z* 509.03, found *m/z* 509.25; calcd for [**1**-Cl^-]$^+$ *m/z*: 1053.52, found *m/z* 1054.75. Elemental analysis (%): Calcd for $Ru_2C_{48}H_{56}N_8Cl_4$•CH_2Cl_2•3H_2O C 47.93, H 5.25, N 9.13; found C 48.11, H 5.31, N 9.02.

Synthesis of [Ru_2(η^6-*p*-cymene)$_2$(*m*-bib)$_2Cl_2$](CF_3SO_3)$_2$ (2)

To a solution of [$RuCl_2$(η^6-*p*-cymene)]$_2$ (61.2 mg, 0.1 mmol) in CH_2Cl_2 (15 mL), a solution of $AgCF_3SO_3$ (51.4 mg, 0.2 mmol) in EtOAc (5 mL) was added. The mixture was further stirred for 2 h at room temperature, the AgCl precipitate was removed by filtration, and *m*-bib (47.8 mg, 0.2 mmol) was added to the resulting solution. The resulting mixture was stirred at RT for another 12 h, and then the solvent was removed on a rotary evaporator. The residue was recrystallized from $CHCl_3$ to give yellow crystals (41.1 mg, yield 33.1%). ^{1}H NMR ($CDCl_3$, 400 MHz) δ: 8.59 (2H, s, H_{im}), 8.42 (2H, s, H_{im}), 7.58 (2H, s, H_{im}), 7.41 (4H, d, H_{im}), 7.07 (2H, m, H_{im}), 6.87 (4H, m, H_{bz}, *m*-bib), 6.73 (2H, d, H_{bz}, *m*-bib), 6.44 (2H, d, H_{bz}, *m*-bib) 5.82 (4H, d, H_{bz}, *p*-cymene), 5.70 (4H, d, H_{bz}, *p*-cymene), 5.24 (4H, d, CH_2), 4.96 (4H, d, CH_2), 2.54 (2H, m, CH), 1.91 (6H, s, CH_3), 1.20 (12H, d, CH_3). ESI-MS(+): calcd for [**2**-2$CF_3SO_3^-$]$^{2+}$ *m/z* 509.03, found *m/z* 509.25; calcd for [**2**-$CF_3SO_3^-$]$^+$ *m/z* 1167.14, found *m/z* 1166.08. Elemental analysis (%): Calcd for $Ru_2C_{50}H_{56}N_8Cl_2F_6S_2O_6$ C 45.63, H 4.29, N 8.51; found C 45.34, H 4.43, N 8.05.

Synthesis of [Ru_2(η^6-*p*-cymene)$_2$(*m*-bib)$_2Cl_2$](SbF_6)$_2$ (3)

To a solution of [Ru_2(η^6-*p*-cymene)$_2$(*m*-bib)$_2Cl_2$](Cl)$_2$ (21.76 mg, 0.02 mmol) in MeOH (5 mL were added 5 mL MeOH solution of $AgSbF_6$ (13.74 mg, 0.04 mmol). The mixture was stirred at room temperature for 2 h, and then the solvent was removed on a rotary evaporator. The residue was recrystallized from $CHCl_3$ to give yellow crystals (11.3 mg, yield 37.9%). ^{1}H NMR ($CDCl_3$, 400 MHz) δ: 9.41 (2H, s, H_{im}), 9.26 (2H, s, H_{im}), 8.15 (2H, s, H_{im}), 7.49 (4H, d, H_{im}), 6.87 (8H, m, H_{bz}, *m*-bib), 6.53 (2H, d, H_{im}), 5.93 (8H, d, H_{bz}, *p*-cymene), 5.36 (4H, d, CH_2), 5.01 (4H, d, CH_2), 2.52 (2H, m, CH), 1.89 (6H, s, CH_3), 1.17 (12H, d, CH_3). ESI-MS(+): calcd for [**3**-2SbF_6^-]$^{2+}$ *m/z* 509.03, found *m/z* 509.17. Elemental analysis (%): Calcd for $Ru_2C_{48}H_{56}N_8Cl_2Sb_2F_{12}$ C 38.70, H 3.79, N 7.52; found C 38.62, H 3.66, N 7.38.

Synthesis of [Ru_2(η^6-*p*-cymene)$_2$(*m*-bib)$_2Cl_2$](NO_3)$_2$ (4)

To a solution of [Ru_2(η^6-*p*-cymene)$_2$(*m*-bib)$_2Cl_2$](Cl)$_2$ (21.76 mg, 0.02 mmol) in MeOH (5 mL) were added 5 mL MeOH solution of $AgNO_3$ (6.79 mg, 0.04 mmol). The mixture was stirred at room temperature for 2 h, and then the solvent was removed under reduced pressure. Purification by flash column chromatography with CH_2Cl_2/MeOH afforded the product as a yellow solid (10.2 mg, yield 44.6%). ^{1}H NMR ($CDCl_3$, 400 MHz) δ: 8.85 (2H, s, H_{im}), 8.74 (2H, s, H_{im}), 7.58 (2H, s, H_{im}), 7.41 (4H, d, H_{im}), 6.90 (8H, m, H_{bz}, *m*-bib), 6.61 (2H, d, H_{im}), 5.85 (4H, d, H_{bz}, *p*-cymene), 5.73 (4H, d, H_{bz}, *p*-cymene), 5.27 (4H, d, CH_2), 4.97 (4H, d, CH_2), 2.56 (2H, m, CH), 1.89 (6H, s, CH_3), 1.18 (12H, d, CH_3). ESI-MS(+): calcd for [**4**-

$2NO_3^-]^{2+}$ *m/z* 509.03, found *m/z* 509.08. Elemental analysis (%): Calcd for $Ru_2C_{48}H_{56}N_{10}Cl_2O_6 \cdot CH_2Cl_2 \cdot H_2O$ C 47.27, H 4.86, N 11.25; found: C 46.82, H 4.81, N 11.16.

Synthesis of [$Ru_2(\eta^6$-*p*-cymene)$_2$(*m*-bib)$_2$Br$_2$](Br)$_2$ (5)

A solution of [$Ru_2(\eta^6$-*p*-cymene)$_2$(*m*-bib)$_2$Cl$_2$](Cl)$_2$ (43.52 mg, 0.04 mmol) in MeOH (5 mL) was stirred at room temperature for 30 min. A solution of KBr (50 equiv, 238 mg) in MeOH (15 mL) was added dropwise to the mixture and stirred for another 24 h. The solvent was removed under reduced pressure. The residue was subsequently purified by silica gel chromatography to give yellow solid (21.8 mg, yield 43.0%). ^{1}H NMR (DMSO, 400 MHz) δ: 8.64 (2H, s, H_{im}), 8.19 (2H, s, H_{im}), 7.51 (2H, s, H_{im}), 7.18 (8H, m, H_{bz}, *m*-bib), 7.09 (4H, d, H_{im}), 6.93 (2H, m, H_{bz}, *m*-bib), 6.03 (4H, d, H_{bz}, *p*-cymene), 5.78 (4H, d, H_{bz}, *p*-cymene), 5.20 (8H, d, CH_2), 2.66 (2H, m, CH), 1.74 (6H, s, CH_3), 1.11 (12H, d, CH_3). ESI-MS(+): calcd for [**5**-2Br$^-$]$^{2+}$ *m/z* 553.49, found *m/z* 553.33. Elemental analysis (%): Calcd for $Ru_2C_{48}H_{56}N_8Br_4 \cdot 3H_2O$ C 43.65, H 4.73, N 8.48; found C 43.76, H 4.95, N 8.44.

Synthesis of [$Ru_2(\eta^6$-*p*-cymene)$_2$(*m*-bib)$_2$I$_2$](I)$_2$ (6)

A solution of [$Ru_2(\eta^6$-*p*-cymene)$_2$(*m*-bib)$_2$Cl$_2$](Cl)$_2$ (43.52 mg, 0.04 mmol) in MeOH (5 mL) was stirred at room temperature for 30 min. A solution of KI (50 equiv, 332 mg) in MeOH (15 mL) was added dropwise to the mixture and stirred for another 24 h. The solvent was removed under reduced pressure. The residue was recrystallized with $CHCl_3$ to give yellow crystals (23.1 mg, yield 39.6%). ^{1}H NMR (DMSO, 400 MHz) δ: 8.26 (2H, s, H_{im}), 8.19 (2H, s, H_{im}), 7.51 (2H, s, H_{im}), 7.18 (8H, m, H_{bz}, *m*-bib), 7.09 (4H, d, H_{im}), 6.93 (2H, m, H_{bz}, *m*-bib), 6.03 (4H, d, H_{bz}, *p*-cymene), 5.78 (4H, d, H_{bz}, *p*-cymene), 5.20 (8H, d, CH_2), 2.66 (2H, m, CH), 1.74 (6H, s, CH_3), 1.11 (12H, d, CH_3). ESI-MS(+): calcd for [**6**-2I$^-$]$^{2+}$ *m/z* 600.48, found *m/z* 601.17. Elemental analysis (%): Calcd for $Ru_2C_{48}H_{56}N_8I_4 \cdot 2H_2O$ C 38.67, H 4.06, N 7.52; found C 38.78, H 4.30, N 7.37.

Synthesis of [$Ru_2(\eta 6$-*p*-cymene)$_2$(*p*-bib)$_2$Cl$_2$](Cl)$_2$ (7)

To a solution of [$RuCl_2(\eta^6$-*p*-cymene)]$_2$ (61.2 mg, 0.1 mmol) in MeOH (15 mL), the ligand *p*-bib (47.8 mg, 0.2 mmol) was added. The reaction mixture was stirred at 338 K for 6 h, the solvent was then removed under reduced pressure. The residue was subsequently purified by silica gel chromatography to give yellow solid (45.7 mg, yield 41.9%). ^{1}H NMR ($CDCl_3$, 400 MHz) δ: 9.74 (4H, d, H_{im}), 7.39 (4H, d, H_{im}), 7.06 (8H, d, H_{bz}, *p*-bib), 6.58 (4H, s, H_{im}), 5.82 (8H, d, H_{bz}, *p*-cymene), 5.69 (4H, d, CH_2), 4.89 (4H, d, CH_2) 2.44 (2H, m, CH), 1.85 (6H, s, CH_3), 1.17 (12H, m, CH_3). ESI-MS(+): calcd for [**7**-2Cl]$^{2+}$ *m/z* 509.03, found *m/z* 509.33; calcd for [**7**-Cl]$^+$ *m/z* 1053.52, found *m/z* 1053.75. Elemental analysis (%): Calcd for $Ru_2C_{48}H_{56}N_8Cl_4 \cdot CH_2Cl_2 \cdot 2H_2O$ C 49.38, H 5.07, N 9.40; found C 48.94, H 5.37, N 9.36.

Synthesis of [$Ru_2(\eta^6$-*p*-cymene)$_2$(*p*-bib)$_2$Cl$_2$](CF$_3$SO$_3$)$_2$ (8)

To a solution of [$RuCl_2(\eta^6$-*p*-cymene]$_2$ (61.2 mg, 0.1 mmol) in CH_2Cl_2 (15 mL), a solution of $AgCF_3SO_3$ (51.38 mg, 0.2 mmol) in EtOAc (5 mL) was added. The resulting mixture was stirred at room temperature for 2 h, the AgCl precipitate was then removed by filtration. The ligand *p*-bib (47.8 mg, 0.2 mmol) was added to the resulting solution. The mixture was stirred at RT for another 6 h, and then the solvent was removed on a rotary evaporator. The residue was recrystallized from $CHCl_3$ to give yellow crystals (43.0 mg, yield 32.6%). ^{1}H NMR ($CDCl_3$, 400 MHz) δ: 8.63 (4H, d, H_{im}), 7.37 (4H, d, H_{im}), 7.04 (8H, d, H_{bz}, *p*-bib), 6.71 (4H, s, Hi_m), 5.77 (4H, d, H_{bz}, *p*-cymene), 5.65 (4H, d, CH_2), 5.54 (4H, d, CH_2), 4.94 (4H, d, CH_2), 2.49 (2H, m, CH), 1.84 (6H, s, CH_3), 1.13 (12H, m, CH_3). ESI-MS(+): calcd for [**8**-2$CF_3SO_3^-$]$^{2+}$ *m/z* 509.03, found *m/z* 509.33; calcd for [**8**-$CF_3SO_3^-$]$^+$ *m/z* 1167.14, found *m/z* 1166.00. Elemental analysis (%): Calcd for $Ru_2C_{50}H_{56}N_8Cl_2F_6S_2O_6$ C 45.63; H 4.29, N 8.51; found C 45.23, H 4.26, N 8.24.

[$Ru_2(\eta^6$-*p*-cymene)$_2$(*p*-bib)$_2$Cl$_2$](SbF$_6$)$_2$ (9)

To a solution of [$Ru_2(\eta^6$-*p*-cymene)$_2$(*p*-bib)$_2$Cl$_2$](Cl)$_2$ (21.76 mg, 0.02 mmol) in MeOH (5 mL), a solution of $AgSbF_6$ (13.74 mg, 0.04 mmol) in MeOH (5 mL) was added. The mixture was stirred at room temperature for 2 h, and then the solvent was removed on a rotary evaporator. The residue was recrystallized from $CHCl_3$ to give yellow solid (12.1 mg, yield 40.6%). ^{1}H NMR ($CDCl_3$, 400 MHz) δ: 7.97 (4H, d, H_{im}), 7.30 (4H, d, H_{im}), 6.95 (8H, d, H_{bz}, *p*-bib), 6.84 (4H, s, Hi_m), 5.74 (4H, d, H_{bz}, *p*-cymene), 5.54 (4H, d, H_{bz}, *p*-cymene), 5.31 (4H, d, CH_2), 4.97 (4H, d, CH_2), 2.57 (2H, m, CH), 1.86 (6H, s, CH_3), 1.19 (12H, m, CH_3). ESI-MS(+): calcd for [**9**-2SbF_6^-]$^{2+}$ *m/z* 509.03, found *m/z* 509.25. Elemental analysis (%): Calcd for $Ru_2C_{48}H_{56}N_8Cl_2Sb_2F_{12}$ C 38.70, H 3.79, N 7.52; found: C 38.45, H 3.67, N 7.42.

Synthesis of [$Ru_2(\eta^6$-*p*-cymene)$_2$(*p*-bib)$_2$Cl$_2$](NO$_3$)$_2$ (10)

To a solution of [$Ru_2(\eta^6$-*p*-cymene)$_2$(*p*-bib)$_2$Cl$_2$](Cl)$_2$ (21.76 mg, 0.02 mmol) in MeOH (5 mL), a solution of $AgNO_3$ (6.79 mg, 0.04 mmol) in MeOH (5 mL) was added. The mixture was stirred at room temperature for 2 h, and then the solvent was removed on a rotary evaporator. The residue was purified by flash column chromatography with CH_2Cl_2/CH_3OH as elution mixture to afford yellow solid (10.6 mg, yield 46.4%). ^{1}H NMR ($CDCl_3$, 400 MHz) δ: 8.83 (4H, d, H_{im}), 7.34 (4H, d, H_{im}), 6.98 (8H, d, H_{bz}, *p*-bib), 6.68 (4H, d, Hi_m), 5.76 (4H, d, H_{bz}, *p*-cymene), 5.64 (4H, d, H_{bz}, *p*-cymene), 5.48 (4H, d, CH_2), 4.90 (4H, d, CH_2) 2.47 (2H, m, CH), 1.81 (6H, s, CH_3), 1.16 (12H, m, CH_3). ESI-MS(+): calcd for [**10**-2NO_3^-]$^{2+}$ *m/z* 510.25, found *m/z* 509.03. Elemental analysis (%): Calcd for $Ru_2C_{48}H_{56}N_{10}Cl_2O_6 \cdot CH_2Cl_2$ C 47.97, H 4.76, N 11.42; found C 47.78, H 4.90, N 11.78.

Synthesis of [$Ru_2(\eta^6$-*p*-cymene)$_2$(*p*-bib)$_2$Br$_2$](Br)$_2$ (11)

A solution of [$Ru_2(\eta^6$-*p*-cymene)$_2$(*p*-bib)$_2$Cl$_2$](Cl)$_2$ (43.52 mg, 0.04 mmol) in MeOH (5 mL) was stirred at room temperature for 30 min, a solution of KBr (50 equiv, 238 mg) in MeOH (15 mL) was added dropwise, and the mixture was stirred for another 24 h. The solvent was removed under reduced pressure. The residue was purified by flash column chromatography to give yellow solid (21.6 mg, 42.7%). ^{1}H NMR (DMSO, 400 MHz) δ: 8.03 (4H, d, H_{im}), 7.34 (4H, d, H_{im}), 7.14 (4H, d, Hi_m), 7.06 (8H, d, H_{bz}, *p*-bib), 5.96 (4H, d, H_{bz}, *p*-cymene), 5.71 (4H, d, H_{bz}, *p*-cymene), 5.22 (8H, d, CH_2), 2.64 (2H, m, CH), 1.80 (6H, s, CH_3), 1.11 (12H, m, CH_3). ESI-MS(+): calcd for [**11**-2Br$^-$]$^{2+}$ *m/z* 553.49, found *m/z* 553.75. Elemental analysis (%): Calcd for $Ru_2C_{48}H_{56}N_8Br_4 \cdot 3H_2O$ C 43.65, H 4.73, N 8.48; found C 43.55, H 4.74, N 8.35.

Synthesis of [$Ru_2(\eta^6$-*p*-cymene)$_2$(*p*-bib)$_2$I$_2$](I)$_2$ (12)

A solution of [$Ru_2(\eta^6$-*p*-cymene)$_2$(*p*-bib)$_2$Cl$_2$](Cl)$_2$ (43.52 mg, 0.04 mmol) in MeOH (5 mL) was stirred at room temperature for 30 min, a solution of KI (50 equiv, 332 mg) in MeOH (15 mL) was added dropwise, and the mixture was stirred for another 24 h. The solvent was removed under reduced pressure. The residue was purified by flash column chromatography to give yellow solid (23.4 mg, 40.2%). ^{1}H NMR (DMSO, 400 MHz) δ: 8.03 (4H, d, H_{im}), 7.32 (4H, d, H_{im}), 7.18 (4H, d, Hi_m), 7.08 (8H, d, H_{bz}, *p*-bib), 6.09 (4H, d, H_{bz}, *p*-cymene), 5.75 (4H, d, H_{bz}, *p*-cymene), 5.20 (8H, d, CH_2), 2.71 (2H, m, CH), 1.72 (6H, s, CH_3), 1.12 (12H, m, CH_3). ESI-MS(+): calcd for [**12**-2I$^-$]$^{2+}$ *m/z* 600.48, found *m/z* 601.25. Elemental analysis (%): Calcd for $Ru_2C_{48}H_{56}N_8I_4 \cdot 2H_2O$ C 38.67, H 4.06, N 7.52; found C 38.67, H 4.32, N 7.34.

Determination of X-ray Crystal Structure

Single-crystal X-ray diffraction data were measured at 296(2) K for complexes **2**, **3**, **6** and at 298 K for complex **8** on a Bruker Apex II CCD using Mo Kα radiation (*λ*= 0.71073 Å). An empirical absorption correction was applied to the data by using the SADABS program. The structures were solved by direct methods and refined by full-matrix least-squares methods with SHELX.[32] All non-hydrogen atoms were refined anisotropically and hydrogen atoms of organic molecule were placed in calculated positions, assigned isotropic thermal parameters, and allowed to ride their parent atoms. The following computer programs and hardware were used: structure solution, SHELXS-*2014/7*; structure refinement, SHELXL-*2014/7*. Data collection parameters and structure refinement details are given in Table S1 in the supporting information. CCDC 1502211 (for **2**), 1502212 (for **3**), 1502213 (for **6**), 1502214 (for **8**) containing the supplementary crystallographic data for this paper that can be obtained free of charge from The Cambridge Crystallographic Data Centre.

Gel Electrophoresis Experiments

The closed circular supercoiled pBR322 plasmid DNA was used for the gel electrophoresis experiments, which was purchased from Sangon Biotech (Shanghai, China). DNA (1 *μ*L, 10 *μ*M) was treated with 4 *μ*L ultrapure water, 5 *μ*L PBS buffer (100 mM) and 10 *μ*L different concentrations of complexes (molar ratio of [M]/[DNA] r_i = 1, 2, 3, 4, 5, 6). The mixture was incubated at 310 K for 12 h in the dark, then 4 μL loading buffer (0.05% Bromophenol Blue, 30 mM EDTA, 36% glycerol, 0.05% Xylene Cyanol FF) was added. Electrophoresis was carried out in a native agarose gel (1%) in 1×TAE buffer for 2 h at 70 mA. The gel was subsequently stained with 1 *μ*g/mL ethidium bromide and visualized under a UV transilluminator and photographed using a digital camera.

Acknowledgements

We thank the Key International (Regional) Joint Research Program of NSFC (Grant No. 21420102002), NSFC (Project 21171095, 21302094,21401105), the Priority Academic Program Development of Jiangsu Higher Education Institutions (PAPD), the "Summit of the Six Top Talents" Program of Jiangsu Province China, ERC (Grant 247450), EPSRC (Grant EP/F034210/1), Science City (ERDF/AWM) for their support, our collaborators for their contributions, and members of EC COST Action CM1105 for stimulating discussions.

Keywords: Organometallic • Coordination complexes • Ruthenium arene • Metallamacrocycles • DNA • anticancer

[1] a) H. K. Liu, P. J. Sadler, *Acc. Chem. Res*. **2011**, *44*, 349-359; b) J. J. Soldevila-Barreda and P. J. Sadler, *Curr. Opin. Chem. Biol*. **2015**, *25*, 172–183.

[2] a) Z. Liu and P. J. Sadler, *Acc. Chem*. *Res*. **2014**, *47*, 1174−1185; b) B. S. Murray, L. Menin, R. Scopelliti and P. J. Dyson, *Chem. Sci.* **2014**, *5*, 2536.

[3] a) H. K. Liu, J. A. Parkinson, J. Bella, F. Wang, P. J. Sadler, *Chem. Sci.* **2010**, *1*, 258-270; b) T. Storr, K. H. Thompson and C. Orvig, *Chem. Soc .Rev.* **2006**, *35*, 534-544.

[4] a) N. P. E. Barry, A. Pitto-Barry, A. M. Sanchez, A. P. Dove, R. J. Procter, J. J. Soldevila-Barreda, N. Kirby, I. Hands-Portman, C. J. Smith, R. K. O'Reilly, R. Beanland, P. J. Sadler, *Nature Commun*. **2014,** *5*, 3851; b) N. P. E. Barry, P. J. Sadler, *Chem. Soc. Rev.* **2012**, *41,* 3264–3279; c) S. H. van Rijt and P. J. Sadler, *Drug. Discov. Today.* **2009**, *14*, 1089-1097.

[5] L. Kelland, *Nat. Rev. Cancer*. **2007**, *7*, 573-584.

[6] A. F. Peacock and P. J. Sadler, *Chem. Asian. J.* **2008**, *3*, 1890-1899.

[7] H. Chen, J. A. Parkinson, R. E. Morris, P. J. Sadler, *J. Am. Chem. Soc.*, **2003**, *125*, 173-186.

[8] H. Chen, J. A. Parkinson, S. Parsons, R. A. Coxall, R. O. Gould, P. J. Sadler, *J. Am. Chem. Soc.* **2002**, *124*, 3064-3082.

[9] C. G. Hartinger, S. Zorbas-Seifried, M. A. Jakupec, B. Kynast, H. Zorbas and B. K. Keppler, *J. Inorg. Biochem.* **2006**, *100*, 891-904.

[10] a) I. Bratsos, D. Urankar, E. Zangrando, P. Genova-Kalou, J. Kosmrlj, E. Alessio and I. Turel, *Dalton Trans.* **2011**, *40*, 5188-5199; b) T. S. Kamatchi, N. Chitrapriya, H. Lee, C. F. Fronczek, F. R. Fronczek and K. Natarajan, *Dalton Trans.* **2012**, *41*, 2066-2077.

[11] a) S. Betanzos-Lara, O. Novakova, R. J. Deeth, A. M. Pizarro, G. J. Clarkson, B. Liskova, V. Brabec, P. J. Sadler and A. Habtemariam, *J. Biol. Inorg. Chem.* **2012**, *17*, 1033-1051; b) A. Levina, A. Mitra and P. A. Lay, *Metallomics* **2009**, *1*, 458-470.

[12] a) P. Govender, A. K. Renfrew, C. M. Clavel, P. J. Dyson, B. Therrien and G. S. Smith, *Dalton Trans.* **2011**, *40*, 1158-1167; b) I. Romero-Canelon, L. Salassa and P. J. Sadler, *J. Med. Chem.* **2013**, *56*, 1291-1300.

[13] R. Pettinari, F. Marchetti, C. Pettinari, A. Petrini, B. W. Skelton, A. H. White, L. Bonfili, M. Cuccioloni and A. M. Eleuteri, *J. Organomet. Chem.* **2015**, *791*, 1-5.

[14] a) P. Elumalai, Y. J. Jeong, D. W. Park, D. H. Kim, H. Kim, S. C. Kang and K. W. Chi, *Dalton Trans.* **2016**, *45*, 6667-6673; b) F. Wang, A. Habtemariam, E. P. van der Geer, R. Fernandez, M. Melchart, R. J. Deeth, R. Aird, S. Guichard, F. P. Fabbiani, P. Lozano-Casal, I. D. Oswald, D. I. Jodrell, S. Parsons and P. J. Sadler, *Proc. Natl. Acad. Sci. U S A.* **2005**, *102*, 18269-18274.

[15] R. Esteghamat-Panah et al., *Inorg. Chim. Acta* (**2016**), http://dx.doi.org/10.1016/j.ica.2016.04.037

[16] X. Li, K. Heimann, X. T. Dinh, F. R. Keene and J. G. Collins, *Mol. BioSyst*., **2016**, *12*, 3032--3045.

[17] a) H. K. Liu, F. Wang, J. A. Parkinson, J. Bella, P. J. Sadler, *Chem. Eur. J*. **2006**, *12*, 6151-6165; b) Y. Fu, M. J. Romero, L. Salassa, X. Cheng, A. Habtemariam, G. J. Clarkson, I. Prokes, A. Rodger, G. Costantini and P. J. Sadler, *Angew. Chem. Int. Ed.* **2016**, *55*, 8909-8912.

[18] a) V. Vajpayee, Y. J. Yang, S. C. Kang, H. Kim, I. S. Kim, M. Wang, P. J. Stang and K. W. Chi, *Chem. Commun.* **2011,** *47,* 5184–5186; b) T. Bugarcic, A. Habtemariam, R. J. Deeth, F. P. Fabbiani, S. Parsons and P. J. Sadler, *Inorg. Chem.* **2009**, *48*, 9444-9453.

[19] a) H. K. Liu, P. J. Sadler, *In Interactions of metallodrugs with DNA in NMR of Biomolecules: Towards Mechanistic Systems*, *Vol. 16* (Eds.: I. Bertini, K. McGreevy), Wiley-VCH, **2012**, pp. 282-296; b) P. Liu, B. Y. Wu, J. Liu, Y. C. Dai, Y. J. Wang and K. Z. Wang, *Inorg. Chem.* **2016**, *55*, 1412-1422; c) G. N. Kaluderovic, T. Krajnovic, M. Momcilovic, S. Stosic-Grujicic, S. Mijatovic, D. Maksimovic-Ivanic and E. Hey-Hawkins, *J. Inorg. Biochem.* **2015**, *153*, 315-321.

[20] Q. Wu, K. Zheng, S. Liao, Y. Ding, Y. Li and W. Mei, *Organometallics* **2016**, *35*, 317-326.

[21] G. Suss-Fink, *Dalton Trans.* **2010**, *39*, 1673-1688.

[22] a) H. K. Liu, S. J. Berners-Price, P. J. Sadler, *Angew. Chem. Int. Ed.* **2006**, *45*, 8153-8156; b) Xin Li, Anil K. Gorle, Tracy D. Ainsworth, Kirsten Heimann, Clifford E. Woodward, J. Grant Collins and F. Richard Keene, *Dalton Trans.* **2015***, 44,* 3594–3603.

[23] a) M. R. Gill and J. A. Thomas, *Chem. Soc. Rev.* **2012**, *41*, 3179-3192; b) J. Aldrich-Wright, C. Brodie, E. C. Glazer, N. W. Luedtke, L. Elson-Schwab and Y. Tor, *Chem. Commun.* **2004**, 1018-1019; c) M. Gras, B. Therrien, G. Süss-Fink, O. Zava and P. J. Dyson, *Dalton Trans.* **2010**, *39*, 10305-10313.

[24] a) E. Alcalde, N. Mesquida and L. Pérez-García, *Eur. J. Inorg. Chem.* **2006**, 3988-3996; b) Z.-Z. Yang, B. Yu, H. Zhang, Y. Zhao, G. Ji and Z. Liu, *RSC. Adv.* **2015**, *5*, 19613-19619.

[25] a) Anna F. A. Peacock and P. J. Sadler, *J. Am. Chem. Soc*. **2006**, *128*, 1739-1748; b) Sarah J. Dougan and P. J. Sadler, *PNAS*. **2008**, *105*, 11628–11633.

[26] a) M. V. Keck and S. J. Lippard, *J . Am. Chem. Soc.* **1992,** *114,* 3386-3390; b) A. T. Abraham, X. Zhou, and S. M. Hecht, *J. Am. Chem. Soc.* **1999,** *121,* 1982-1983; c) Z. Zhu, X. Wang, T. Li, S. Aime, P. J. Sadler and Z. Guo, *Angew. Chem. Int. Ed*. **2014**, *53*, 13225-13228.

[27] P. X. Xi, Z. H. Xu, F. J. Chen, Z. Z. Zeng and X. W. Zhang, *J. Inorg. Biochem.* **2009**, *103*, 210-218.

[28] J. V. Mehta, S. B. Gajera, D. B. Raval, V. R. Thakkar and M. N. Patel, *Med. Chem. Commun.* **2016**, *7*, 1617-1627.

[29] G. L. Zhang, H. Y. Zhang, Y. Gao, R. Tao, L. J. Xin, J. Y. Yi, F. Y. Li, W. L. Liu and J. Qiao, *Organometallics* **2014**, *33*, 61−68.

[30] Y. Li, C. P. Tan, W. Zhang, L. He, L. N. Ji and Z. W. Mao, *Biomaterials* **2015**, *39*, 95-104.

[31] K. K. Lo, B. T. Chan, H. W. Liu, K. Y. Zhang, S. P. Li and T. S. Tang, *Chem Commun (Camb)* **2013**, *49*, 4271-4273.

[32] W.-P. Leung, Y.-C. Chan, T.-H. Choi and H.-K. Lee, *Eur. J. Inorg. Chem.* **2016**, 3859–3867.